UNIVERSITY OF CALIFORNIA, SAN DIEGO

DPY-19-1: a Murine Endoplasmic Reticulum Protein that Controls Cortical Migration

A Thesis submitted in partial satisfaction of the requirements for the degree Master of Science

in

Biology

by

Alex Karl Peterson Ohlendorf

Committee in charge:

Professor Yimin Zou, Chair
Professor Shelley Halpain
Professor Yishi Jin

2010

UMI Number: 1477925

All rights reserved

INFORMATION TO ALL USERS
The quality of this reproduction is dependent upon the quality of the copy submitted.

In the unlikely event that the author did not send a complete manuscript
and there are missing pages, these will be noted. Also, if material had to be removed,
a note will indicate the deletion.

UMI 1477925
Copyright 2010 by ProQuest LLC.
All rights reserved. This edition of the work is protected against
unauthorized copying under Title 17, United States Code.

ProQuest LLC
789 East Eisenhower Parkway
P.O. Box 1346
Ann Arbor, MI 48106-1346

The Thesis of Alex Karl Peterson Ohlendorf is approved, and it is acceptable in quality and form for publication on microfilm and electronically:

_____

_____

_____
Chair

University of California, San Diego

2010

TABLE OF CONTENTS

LIST OF FIGURES AND TABLES

ACKNOWLEDGEMENTS

Thank you Yimin Zou and Delphine Delaunay. Without your constant guidance and support, this thesis would not have been possible. A special thank you to all the members of Yimin Zou's lab for all the help you've provided in this endeavor. Also, thank you Mom and Dad for always being there when things couldn't seem any worse.

ABSTRACT OF THE THESIS

DPY-19-1: a Murine Endoplasmic Reticulum Protein that Controls Cortical Migration

by

Alex Karl Peterson Ohlendorf

Master of Science in Biology

University of California, San Diego, 2010

Professor Yimin Zou, Chair

The gene *dpy-19* has been shown to be involved in migration of the developing nervous system in *Caenorhabditis elegans*. We previously have characterized a mouse homologue for this gene. Its expression pattern and association with the *C. elegans* gene suggest a role for it in cortical migration. Deprivation of mouse DPY-19-1 protein *in vitro* results in neurons with fewer processes and unusual membrane

ruffling. We show here that downregulation of *dpy-19-1* during cortical migration leads to an increased rate of migration. Additionally, migrating cells with downregulated *dpy-19-1* might have an abnormally shaped leading process. We use a neurosphere migration assay to further examine the role of *dpy-19-1* in migration, and results so far are inconclusive.

INTRODUCTION

Neuronal migration plays a critical role in the proper development of the nervous system. In development of the cortex, cells can take two main pathways: radial and tangential migration. Radial cell migration starts around embryonic day 12.5 (E12.5), and it involves progenitor cells leaving the ventricular zone and migrating along radial glia out to the cortical plate to form the layers of the cortex. The cortical layers are formed in an "inside-out" manner, meaning that cells migrate past previously formed deeper layers and the more superficial layers are formed later in development. In tangential migration, pre-cortical GABAergic interneurons migrate from the Lateral Ganglionic Eminence (LGE) and the Medial Ganglionic Eminence (MGE) through the cortex at an angle perpendicular to radial migration (Austin and Cepko, 1990; Marin and Rubenstein, 2001; Marin and Rubenstein, 2003).

Genes involved in cell migration show high conservation among species. In *C. elegans*, *dpy-19* regulates the migration of Q neuroblasts (Honigberg and Kenyon, 2000). During development of *C. elegans*, the Q neuroblasts polarize and migrate in either an anterior or posterior direction (Salser and Kenyon, 1992). The posteriorly migrating QL neuroblasts (on the left side of the worm) express homeobox gene *mab-5*, whereas the anteriorly migrating QR neuroblasts do not. Expression of *mab-5* is controlled by Wnt family gene *egl-20* (Harris et al., 1996). Absence of DPY-19 was discovered to cause a defect exclusively in the initial polarization and migration of Q neuroblasts (Chan et al., 1996; Honigberg and Kenyon, 2000). Work by a previous graduate student of this lab uncovered three potential mouse homologues for the *dpy-*

19 gene, named murine *dpy-19-1*, *-2*, and *-3*. The mouse DPY-19-1 has eleven predicted transmembrane domains, which may indicate that it is a multi-spanning transmembrane protein. It is subcellularly expressed at the endoplasmic reticulum and around the nucleus. During development, it is seen expressed in the cortical plate between E12.5 and E18.5, coinciding with cortical radial migration, which suggests that it may play a role in cortical cell migration (King, 2006). I have successfully reproduced the previously shown cortical expression at E14.5 (Fig. 1A), which does not colocalize in the developing cortex with NeuN, a marker for mature neurons (data not shown). I can show similar subcellular localization around centrosomes (Fig. 1B), and colocalization with the endoplasmic reticulum (Fig. 1C).

Attempts have been made to characterize the function of this gene, and to determine if it has a role in the development of the mouse nervous system. Experiments done by this lab on this mammalian *dpy-19-1* gene *in vitro* have hinted at some aspects of its function. Dissociated neuronal cultures from embryos that had been electroporated *ex vivo* with *dpy-19-1* shRNA show that decreased *dpy-19-1* expression results in neurons that develop fewer processes than the shRNA control after 2 days of *in vitro* culture. Additionally, these neurons display unusual membrane kinetics, resulting in sudden "ruffling" of the membrane in a manner that appears unstable and uncoordinated (data not shown). Since the control of neurite dynamics has been shown to be important for migration (Kwiatkowski et al., 2007), and *dpy-19-1* is known to be expressed in the cortex, we wanted to determine whether the downregulation of *dpy-19-1* would cause a defect in the development of cortical cells.

To this end, we examined the effect of *in utero* electroporation of *dpy-19-1* shRNA. We saw that the relative rate of migration was increased in cells that had downregulated *dpy-19-1* expression, and that these cells took on a different morphology. However, these results did not appear to be shown by a neurosphere-based *in vitro* migration assay.

In an attempt to connect membrane ruffling to increased migration speed with *dpy-19-1* downregulation, we used the migration of neurospheres as an *in vitro* assay for migration. Neurospheres are so named because they are a result of repetitive division of free-floating neural stem cells in growth-factor-containing media. Single neural stem cells will give rise to a spherical-shaped mass of neural cells of varying types (Pevny et al., 2003). When neurospheres are placed on coverslips coated with laminin and PDL, cells will begin to migrate outward in all directions. This behavior has been utilized as an assay to show the effect of doublecortin on migration *in vitro* (Ocbina et al., 2006). We used AMAXA nucleofector™ technology to deliver the D1, DR, and PsuperGFP constructs into neurospheres prior to being plated on coverslips (Fig. 2). After a lot of troubleshooting, we were able to consistently generate neurospheres with migrating transfected cells.

MATERIALS AND METHODS

Mouse embryo brain slice sectioning and staining

Mouse embryo brain tissue was dissected, fixed overnight in 4% PFA, washed in PBS, and then equilibrated in 20% sucrose solution at 4°C. Alternatively, *in utero* electroporated embryonic brains were obtained from the lab of Dr. Shimigori, having been electroporated at E12.5, then dissected and fixed at either E14.5 or E16.5, and shipped in PBS. For each adult pregnant mouse, *in utero* electroporation was performed on its embryos using only one of the two shRNA constructs, D1 or DR. Brain tissue samples were embedded in OCT compound and sectioning was performed on a LEICA CM3050 S cryostat. Coronal sections were cut at 10µm or 40µm and mounted on Superfrost PLUS slides. Immunostaining was performed by washing twice with 1X PBS for 5 minutes, blocking with PDT (1X PBS with 1% donkey serum, 2% bovine serum albumin, and 1% tritonase) for 1 hour at room temperature in a humid chamber. Then the slides were incubated overnight with primary antibodies diluted in PDT, using parafilm to cover the slides to minimize the amount of primary antibody needed. Slides were subsequently washed three times in 1X PBS at room temperature for 15 minutes, incubated in secondary antibody diluted in PDT for 1 hour at RT, washed three more times in 1X PBS, stained using 1:25,000 DAPI in ddH_2O for 5 minutes at RT, washed 3 times in 1X PBS for 5 minutes at RT, washed once briefly in ddH_2O, and mounted with Fluoromount-G (SouthernBiotech). Imaging was performed on a ZEISS LSM 510 inverted confocal microscope.

Neurosphere migration assay

The method used in these experiments for neurosphere migration is based mainly on previous studies (Durbec et al., 2008; Ocbina et al., 2006). E14.5 CD1 mice were dissected to remove the lateral cortex dorsal of the Lateral Ganglionic Eminence, removing the more rostral and caudal parts (Fig. 2A). These portions of cortex were dissociated in 1mL of Trypsin EDTA 1x (Mediatech, Inc.) diluted 1:10 in DMEM 1x (Mediatech, Inc.) for 15 minutes at 37°C, and then triturated with a P1000 pipette. Next, 9mL of DMEM with 10% HI FBS (GIBCO) were added to the dissociated cortex, the cells were spun down for 5 minutes at 1000rpm, counted, and added to four 75cm^2 canted neck flasks (Corning) in 25mL of Neurosphere Growth Media (NGM: 1:100 GlutaMax (GIBCO), 1:100 Penicillin/Streptomycin (Mediatech, Inc.), 1:100 N2 (GIBCO), 1:50 B27 (GIBCO), 1:10,000 bFGF (Sigma), 1:10,000 EGF (Sigma)) at a density of 85,000 cells/mL and incubated for 7 days at 37°C (5% CO_2). After the neural stem cells divided for 7 days to produce neurospheres, the contents of the flasks were spun down and counted to make sure there were about 2*10^6 cells per nucleofection in accordance with the AMAXA Mouse Neural Stem Cell Nucleofection protocol (LONZA). The samples were then nucleofected following said protocol using 20µg of DNA (with the exception of pMAXGFP, of which 6µg were used), and were transferred to 6-well plates (Corning, Inc.) with warm NGM to incubate overnight at 37°C. 24 hours after nucleofection, transfected neurospheres of 80-120µm in size were transferred with a P2 pipette to a 4-well plate (Nunclon) containing warm Culture Medium I (as described in the Lonza NSC Nucleofection

protocol so that they could be plated in rapid succession without contamination of other cells from the sample (Fig. 3). Plating of the neurospheres involved transferring them to coverslips coated with PDL (from Millipore, 20µg/mL in ddH_2O overnight at RT) and laminin (from Invitrogen, 25µg/ml in DMEM for 30 minutes at 37°C) in a 24-well plate (Corning, Inc.) with 500µl of Culture Medium II (as described in the Lonza NSC Nucleofection protocol, except without FCS). Images of live neurospheres were taken using a ZEISS Axiovert 40 CFL microscope. After 48 hours, neurospheres were fixed in 4% PFA and stained for immunofluorescence.

Immunostaining neurospheres and dissociated neuronal cultures

Dissociated neurons derived from E13.5 CD1 mouse cortex were plated on coverslips coated with 20µg/mL Poly-D Lysine (PDL) and 10µg/mL laminin, and were cultured in Neurobasal media (Gibco) with 1:100 B27, 40mM glucose, 1:100 GlutaMax, 1:100 Pen/Strep for 48 hours. Staining procedures were the same for coverslips with neurospheres or dissociated neuronal culture cells. First, a wash was performed with 1x PBS; then the cells were fixed with 4% warm PFA for 10 minutes at 37°C. Next, three brief washes were performed using 1x PBS, blocking was performed using 1x PBS with 10% donkey serum and 0.1% tritonase, and primary antibodies were applied after being diluted in the blocking solution. The primary antibodies were left to incubate overnight at 4°C in a humid chamber, after which three more brief washes were performed with 1x PBS, the secondary antibodies were applied for 1 hour at RT once diluted in the blocking solution, three more washes were

performed in 1x PBS, the coverslips were incubated with 1:25,000 DAPI in ddH_2O for 5 minutes at RT, then 3 more washes were performed in 1x PBS, another quick wash in ddH_2O, and the coverslips were mounted using Fluoromount-G (SouthernBiotech).

Generation of shRNA constructs

The *dpy-19-1* shRNA constructs were made by Dr. Delphine Delaunay, and confirmed to work in downregulating *dpy-19-1* expression in vitro (data not shown). The D1 construct causes shRNA expression for downregulating expression of *dpy-19-1*, the DR construct has random shRNA to serve as a control for shRNA expression, and PsuperGFP (PS) is used as a vector control, since it is the basic vector from which these constructs were made. All three constructs induce GFP expression for easy identification of transfected cells.

Antibodies

Centrosomes were stained with mouse anti-gamma-tubulin antibody (Sigma); layer 5 pyramidal neurons were stained with rat anti-Ctip2 (Abcam); neuronal progenitors were stained with mouse anti-Tuj1 (Sigma); radial glia were marked with mouse anti-nestin (BD Biosciences); astrocytes and neural stem cells were marked with rabbit anti-GFAP (Sigma); cell nuclei were stained with DAPI (Sigma); endoplasmic reticulum was revealed using mouse anti-KDEL (Stressgen); D1, DR and Psuper transfected cells were marked with goat anti-GFP; and the DPY-19-1 protein

was marked with an antibody made by Leslie King, a previous lab member (King, 2006).

RESULTS

Downregulation of dpy-19-1 in vivo

To confirm that *in utero* electroporation of D1 shRNA caused a decrease in *dpy-19-1* expression, we examined brain samples that had been electroporated at E12.5 and fixed at E14.5. Electroporation was performed by injecting DNA into the ventricle of the embryo and passing a current through the brain such that the DNA will enter progenitor cells that will give rise to a specific area of the cortex (Fig. 2A). Confirmation of downregulation was performed at E14.5 because it gives an intermediate point between the electroporation at E12.5 and the analysis of migration at E16.5. At this timepoint, to have an effect on migration, D1 needs to be exerting its effect by causing a decreased amount of DPY-19-1 in transfected cells. These E14.5 samples were immunostained for GFP to identify cells that had been transfected, DPY-19-1 to show the level of protein, and were stained with DAPI to visualize the cell nuclei. Slices were cut 10μm thick so that there would be minimal overlap in the DPY-19-1 staining. The downregulation of *dpy-19-1* is immediately apparent in cortical cells expressing the D1 construct (Fig. 4). The usual perinuclear DPY-19-1 is almost completely abolished. Although this experiment was performed only on one litter of mouse embryos, the extent of the downregulation, and the consistent downregulation *in vitro* (data not shown) are taken as indications that the construct is functioning properly.

Regulation of cortical migration by dpy-19-1

Due to the role of *dpy-19* in neuronal migration in *C. elegans* (Honigbert and Kenyon, 2000), and the effects of *dpy-19-1* downregulation on mouse neurons *in vitro*, we hypothesize that the mammalian homologue will have a role in neuronal migration in the *in vivo* mouse cortex. To determine the effect of *dpy-19*-1 downregulation in developing cortices, E12.5 mouse embryos were electroporated *in utero* with D1 and DR constructs. At E16.5 the brains were fixed and sectioned into 40µm thick sections so that most of each cell would be visible for analyzing morphology. These sections were immunostained with rat anti-Ctip2, a marker for layer V pyramidal neurons, to allow computation of a relative distance of migration. In comparison with the control, downregulation of *dpy-19-1* appeared to cause cells to migrate faster relative to the Ctip2 staining (Fig. 5). By making a contour line around the outer edge of this layer, and projecting bands that were half the width of the Ctip2 layer, we were able to divide the migrated cells into subsets based on their position (Fig. 6). The number of cells in each band was reported as a percentage of the cells from that slice, and the percentage of cells in each band was averaged across all slices. The data confirmed the observed increase in migration, as fewer cells expressing D1 occupied the Pre Ctip2 band ($p=0.0007$), and there were more D1 expressing cells in the Second Half of Ctip2 band ($p=0.0009$) (Fig. 7).

Regulation of the leading process by dpy-19-1

Decrease of *dpy-19-1* expression in mouse primary cortical culture causes membrane ruffling, in which sudden and prominent swelling occurs in cytoplasmic volume at locations along the neurites. These cells also have reduced number of processes (unpublished observations). Using the same samples as in the migration study, we saw a similar disruption of neurite function *in vivo*, with unusually serpentine leading processes (Fig. 8A,C). In an effort to quantify this phenotype, we measured the length along the process (Fig. 8B,D, magenta tracing) and divided it by the length between the beginning and end of the process (Fig. 8B,D, blue line), such that processes that took a longer path to reach the destination would show a higher ratio, called here "serpentine index". Cells were counted only if their leading process could be continuously traced back to the nucleus, the process had a direct distance from beginning to end of 30-60μm, and there was no overlap with other cells. These data showed D1 had a significantly higher serpentine index than DR across two rounds (Fig. 8E, $p=0.0016$). However, the difference is not significant if the data from the second round is considered alone.

Effect of dpy-19-1 on neurite formation in the intermediate zone

Recent studies have shown that branching of the leading process can inhibit the speed of migration of cortical neurons. Conversely, decreasing the amount of branching by the leading process can actually increase the rate of migration (Guerrier et al., 2009; Gupta et al., 2003; Ohshima et al., 2007). If downregulation of *dpy-19-1*

causes a decrease of process formation *in vivo* like it does *in vitro*, this would dovetail nicely with the observed result of increased migration from *dpy-19-1* downregulation. Our first thought was to examine the leading process in the E16.5 brains that were sectioned at 40µm for the quantification of migration. However, either the sections had insufficient thickness, or the angle of cutting was too oblique to the plane of the leading processes, because most of the leading processes observed were not long enough to allow observation of their branching patterns. Using the other *in utero* electroporated sample we had available, the E14.5 brains sectioned at 10µm, we examined the branching of multipolar cells in the intermediate zone. Tracings of the cells were made in ImageJ (Fig. 9A). At first observation, D1-positive intermediate zone cells looked like they indeed had fewer processes per cell (Fig. 9B), consistent with an increased speed of migration. However, after more samples were processed, the difference between D1 and DR became much less pronounced, and, in fact, reversed. In Sholl analysis, D1 had more processes at 10 and 12 µm from the center of the cell (Fig. 10, $p=0.0496$, and $p=0.0237$, respectively) but none of the other data points had a significant difference. However, the sample size was quite small (17 cells for D1, 13 cells for DR), so these data are not conclusive. Also, the difference exhibited here may be only as a result of cells with smaller cell bodies being counted for DR, since the trend of the graph indicates that the maximum number of processes for DR peaked at 6µm. The point at which the circle for Sholl analysis is no longer crossing through the cell body would logically be the point at which Sholl analysis detects the most processes, since most of the processes on these cells terminated very

close to the cell body. Again, the thickness of cutting may be a problem here as well, since it is very likely that these 10μm sections do not reveal the entirety of the cell's neurite complexity.

Characterization of migration assay

Untransfected cells exhibit exuberant migration up to 48 hours after being plated (Fig. 11A-D). Processes of these cells can be seen projected from the neurosphere as early as 2 hours after plating (Fig. 11E). Time-lapse imaging of migrating cells reveals that movement occurs by nuclear translocation (Fig. 11 G-J, K-N), similar to how migration occurs in the cortex (Edmondson and Hatten, 1987). However, these cells do not appear to require radial glia to migrate along. Immunohistochemistry reveals that the migrating cells are of varying expression profiles, as revealed by staining for nestin, a radial glial marker (Fig. 12B), GFAP, a marker that stains astrocytes and neural stem cells (Fig. 12C), and Tuj1, a marker for neuron differentiated neural progenitors (Fig. 12E). Many of the migrating cells express *dpy-19-1*, as well (Fig. 12F, 13G).

Effect of dpy-19-1 downregulation on neurosphere migration

Nucleofection™ of pMAXGFP (provided with the AMAXA nucleofection™ kit) generates a sizeable amount of GFP-positive migrating cells (Fig. 13A). By contrast, expression of the pSUPER-based constructs would show only a few GFP positive cells per neurosphere (Fig. 13B-D). Expression of D1 in neurosphere

migratory cells still causes downregulation of *dpy-19-1* expression (Fig. 13G). After 48 hours of migration, the neurospheres were fixed and stained for immunofluorescence. GFP positive migratory cells from each nucleofection™ condition were confirmed using an anti-GFP antibody, and cells were segregated for quantification based on whether they expressed Tuj1 (Fig. 13E-H). Overall, 29.5% of the D1-positive cells from the rounds stained for Tuj1 were also Tuj1-+, 25.6% of DR samples were Tuj1-+, and 37% of the PS. The distance of migration of each GFP-positive cell was determined by calculating the distance travelled from the edge of the neurosphere (Fig. 13C), and these values are shown for either all GFP-positive cells in Figure 13A, or only the Tuj1 positive cells in Figure 13B. The chosen method of data quantification did not show a difference among the different nucleofection conditions, regardless of whether Tuj1 cells were specifically chosen for quantification (Fig. 13A-B). In the raw data the D1 construct had a higher mean migration than the DR in all but one trial for both non-specific (Table 1A) and Tuj1-specific (Table 1B) quantification. However, the PS data showed high amount of variability, indicating that more samples or higher electroporation efficiency might be more ideal for this method (Table 1). Observation of the overall migration of the neurospheres between the different rounds gave no apparent reason for the variability in average migration of transfected cells (data not shown).

DISCUSSION

We have examined here the role of *dpy-19-1* in cortical development. Although most of the data still require replication, these *in vivo* migration and morphology results complement previous findings by this lab showing morphological disturbances via expression of *dpy-19-1* shRNA *in vitro*. We hope to replicate these results in additional samples, providing stronger evidence for the role of mammalian *dpy-19-1* in cortical development. However, there are still some issues with the results of these experiments that need to be addressed.

Cells with downregulation of *dpy-19-1* during cortical migration *in vivo* appear to have faster migration. This result is surprising, because in *C. elegans* an absence of DPY-19 causes polarization defects and temporary halting of migration. One could attribute these different effects of *dpy-19* homologue downregulation to the differences in the organisms. A major caveat of the migration of D1 and DR neurons *in vivo* is that D1 had a visibly stronger expression than DR (Fig. 3). Since the presence of electroporated cells was determined by examination of the GFP signal, and some of the electroporated cells were only slightly more intense than the background, it is possible that the high expression of GFP from D1-positive cells could have resulted in a misrepresentative higher cell count in dense areas of the brain, like the cortex. These experiments need to be reproduced in conditions of roughly equivalent D1 and DR expression. To carry this work forward, additional timepoints could be used to see the eventual fate of D1 vs. DR cells, and to see if the D1-positive migrating cells are still targeted to the correct area when they conclude radial

migration. Additionally, a knockout mouse should be generated to show the effects of elimination of DPY-19-1 on a larger scale.

In terms of the morphological effects of *dpy-19-1* downregulation *in vivo*, there are still alternate means to more fully explore and visualize any changes. Since one problem with the chosen method of exploration was the possibility of processes being truncated when cryostat sections were taken, an alternative method would be to use cortical slice cultures to study migration (Haydar et al., 1999). This method would give living neurons a chance to form processes, allowing observation of fully developed processes and the effect thereon of *dpy-19-1* downregulation. Additionally, cortical slice cultures would allow live imaging of migration, to observe differences in the morphology of cells with downregulated *dpy-19*-1. An issue that must be addressed about the observed difference in leading process morphology caused by -*dpy-19-1* downregulation is that in the first round of samples that were quantified, in which the difference was first observed, the cortex had massive signs of damage (data not shown). In the subsequent round that was quantified, the slices of cortex had a much healthier and more intact appearance, and although the trend of increased serpentine index with D1 still existed, the difference from DR was not significant. Thus, this result must be satisfactorily reproduced before it can be considered as true.

With regards to the neurosphere migration assay, *dpy-19-1* downregulation did not appear to cause the same the overmigration phenotype seen with *dpy-19-1* downregulation *in vivo*. There are several possible reasons for this. First, it may be an error in the method that was used to quantify the data. Looking at the position of cells

after 48 hours is not necessarily the best method of quantifying speed of migration. Cells that only just began migrating would skew the data towards slower migration, regardless of how fast individual cells are migrating. An alternative method would be to take two sets of pictures a few hours apart and compare how much cells move in that interval. In my attempts to use this method, it appears that a difference of 6 hours is too much, because the cells are not necessarily consistently migrating straight outward, and it is easy to lose track of migrating neurons after a short time. Another part of this assay that is not ideal is the lack of a proven positive control for overmigration. A neurosphere migration assay has been used to show that knockdown of doublecortin decreases migration from this neurosphere, but when doublecortin was overexpressed, there was no overmigration phenotype (Ocbina et al., 2006), despite overmigration occurring in a cerebellar granule cell migration assay with overexpression of Doublecortin (Tanaka et al., 2004). Typically, neurosphere migration assay has been used to study the effects of changing components of the media, under which overmigration is possible (Liu et al., 2009). However, it is yet unknown whether this assay can model overmigration through DNA transfection. Finally, it may be that this assay is not suitable for modeling the effect of *dpy-19-1* on radial migration. The neurosphere migration assay has more favorably been compared to chain migration, which occurs in tangential migration (Jacques et al., 1998). It was hypothesized that the instability of membrane dynamics seen *in vitro* with *dpy-19-1* downregulation would be sufficiently impairing to affect cells migrating along coverslips, but the lack of responsiveness of the neurosphere assay may be indicative

that decreased process formation would be a more effective target for understanding the effect of *dpy-19-1* downregulation on migration *in vivo*.

FIGURES AND TABLES

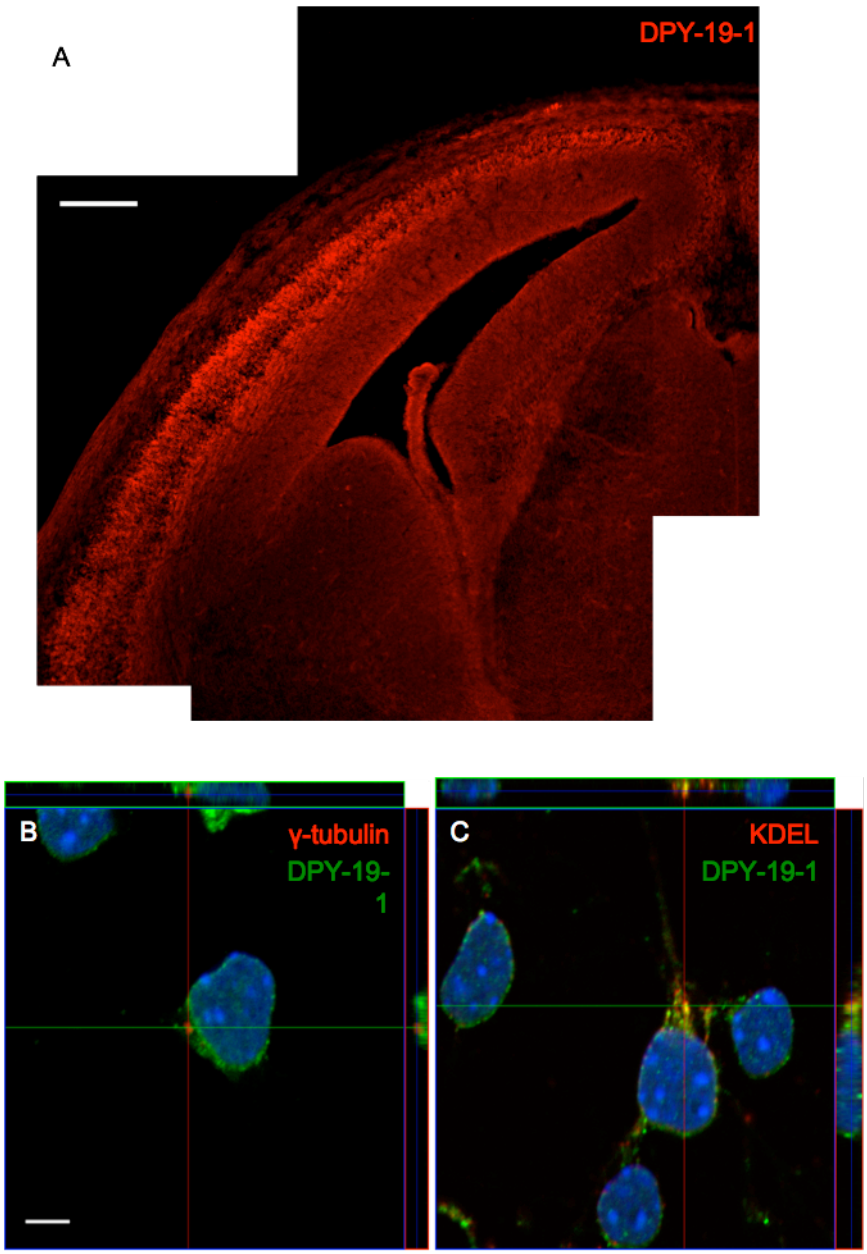

Figure 1. *Characterizing the expression profile of dpy-19-1.* (A) Mouse embryonic brain dissected at E14.5, fixed, embedded in OCT, and sectioned on a cryostat into 20µm sections. Immunostaining was performed against DPY-19-1. Multiple 10x pictures were taken and reconstructed into an image of the entire cortex. Scale bar represents 200µm. (B) Orthographic projection of dissociated neuronal culture stained for gamma-tubulin (red) to visualize the centrosomes, DAPI (blue), and DPY-19-1 (green). (C) The same as in (B) except that samples were stained with KDEL (red) to visualize the endoplasmic reticulum. Neurons were dissociated from mouse CD1 E13.5 brains. Side panels are used to show depth at color-coded slicing planes. (B) has a depth of 1.9µm, (C) has a depth of 2.4µm. Scale bar represents 5µm.

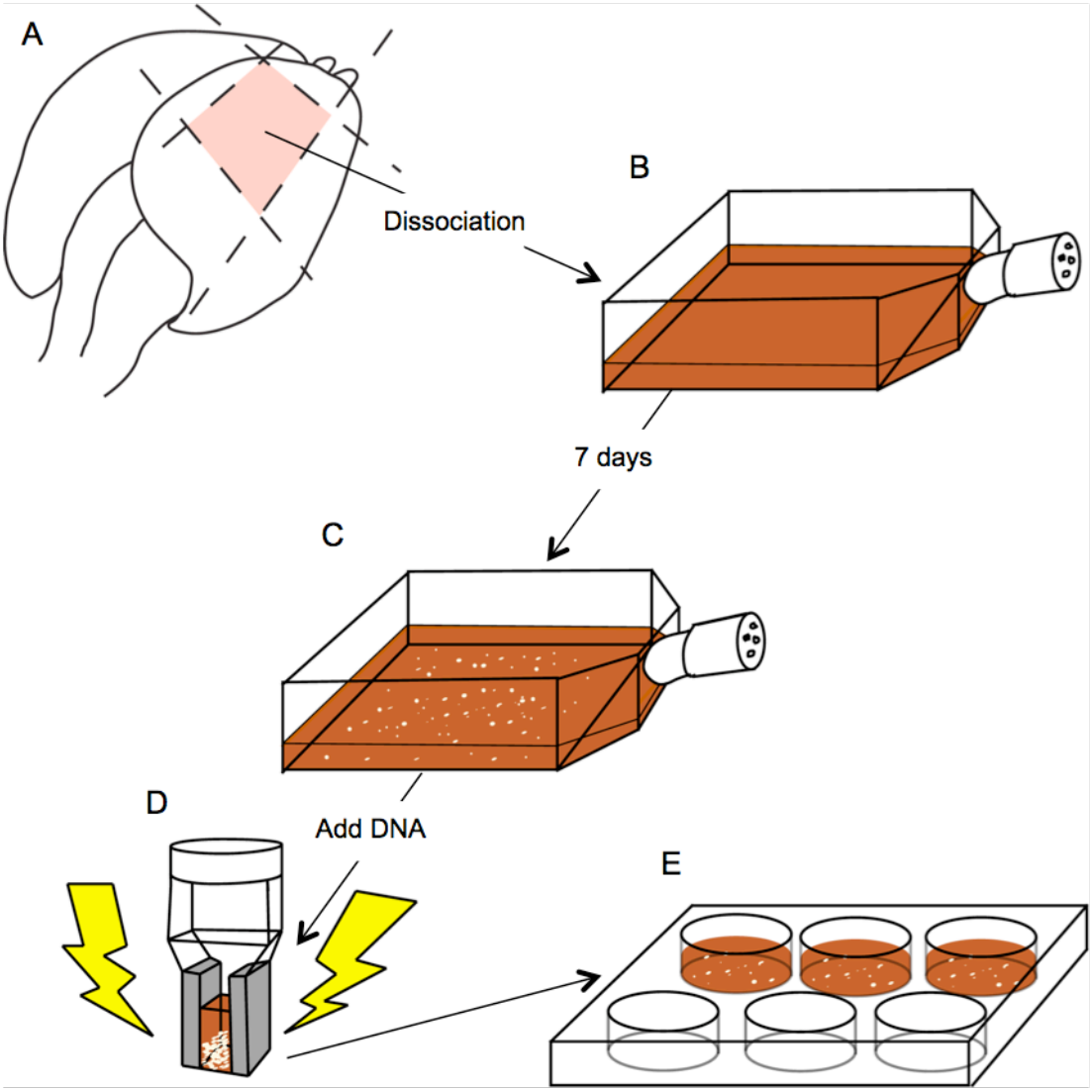

Figure 2. *Illustrative diagram of neurosphere generation and nucleofection™.* First, part of the E14.5 cortex is dissected (A) and dissociated into four 75cm^2 canted neck flasks containing 25mL of NGM at a density of 85,000 cells/mL. These flasks are cultured for 7 days at 37°C and 5% CO_2 to produce neurospheres of varying sizes (C). Neurospheres are nucleofected™ with the different DNA constructs using the LONZA AMAXA Mouse Neural Stem Cell Nucleofection protocol (D), then quickly transferred to warm Culture Medium I (E) for 24 hours of incubation before plating.

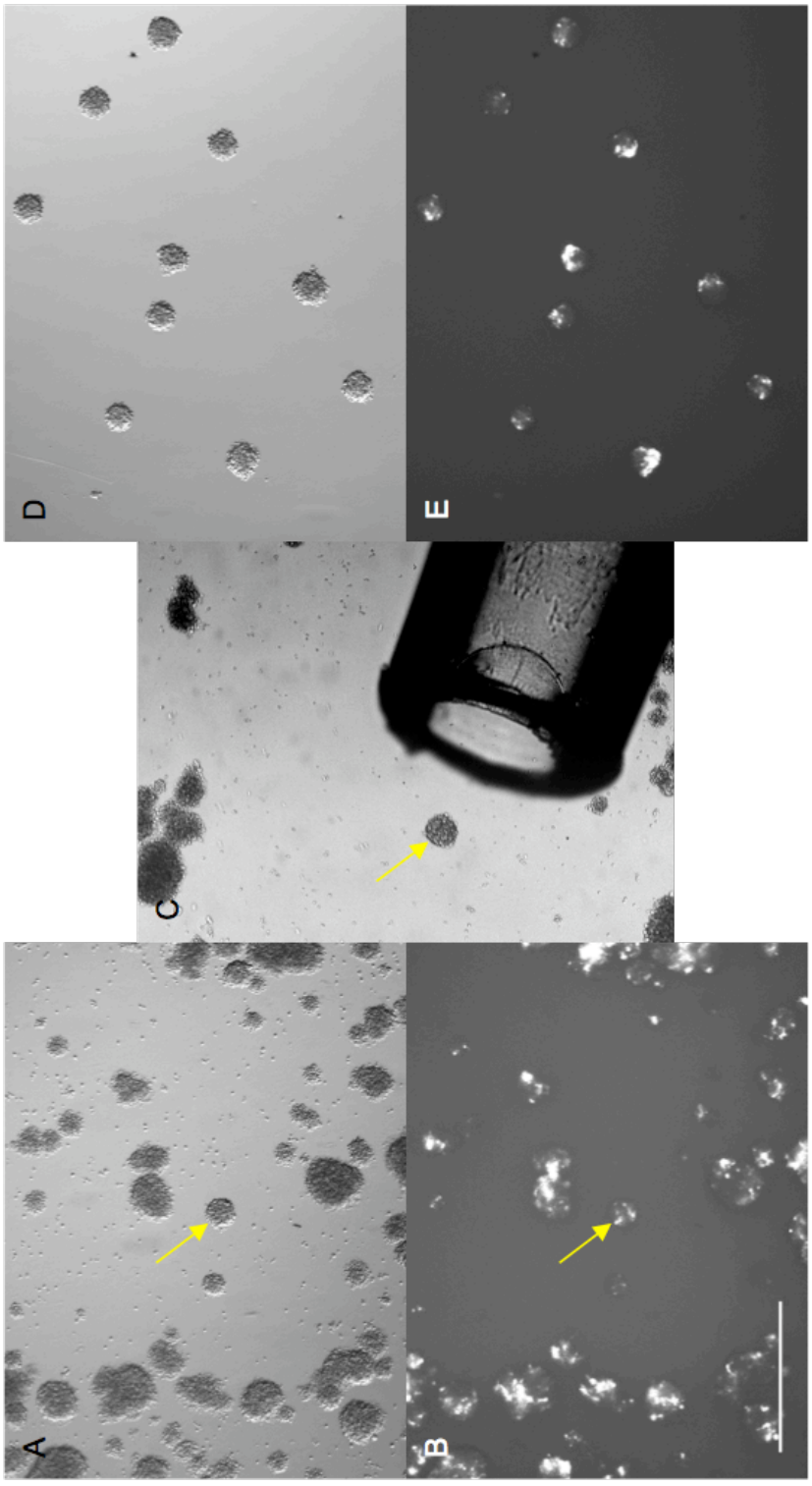

Figure 3. *Selection of neurospheres.* (A) Differential Interference Contrast (DIC) microscopy of Psuper transfected neurospheres. Neurospheres were selected based on healthy appearance with clearly defined edges, size between 80-120µm, and spherical shape (yellow arrow). (B) Fluorescent imaging of GFP. Neurospheres were also selected to have transfected cells (yellow arrow). Scale bar represents 500µm. (C) The area around the neurosphere of interest is cleared, and a P2 micropipette is used to transfer the neurosphere to a 4-well plate. (D-E) Acceptable neurospheres are collected on in a 4-well plate for rapid successive plating.

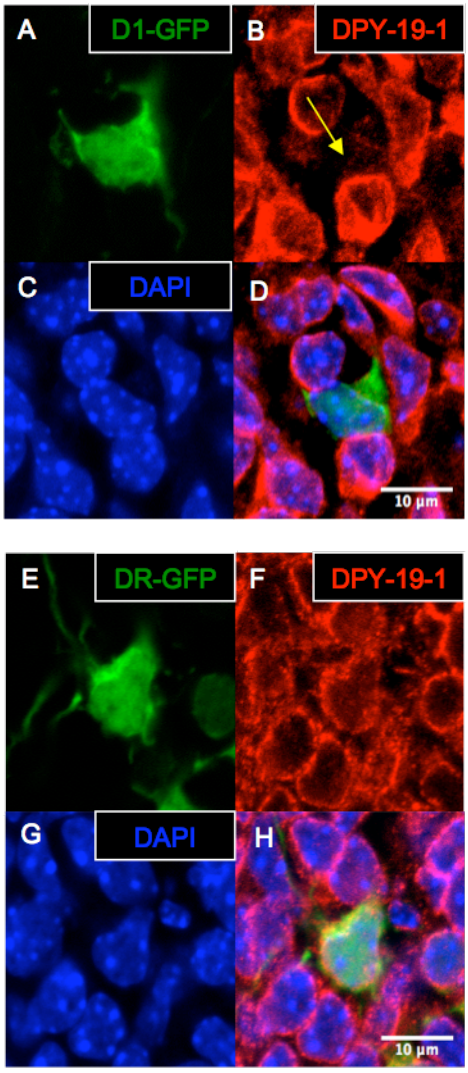

Figure 4. *Downregulation of endogenous dpy-19-1 in cortical neurons using D1 shRNA construct.* Mouse pre-cortical neuronal progenitors were electroporated with D1 or DR constructs *in utero* at E12.5, dissected at E14.5, and fixed. The brains were then cut into 10µm coronal sections on a cryostat, and images were taken of transfected neurons after the slides were processed for immunofluorescence with anti-GFP (green) (A, E), anti-DPY-19-1 (red) (B, F), and DAPI (blue) (C, G). Merged images of all the colors are shown in (D, H). D1-transfected cell showing downregulation of *dpy-19-1* is demarcated with a yellow arrow.

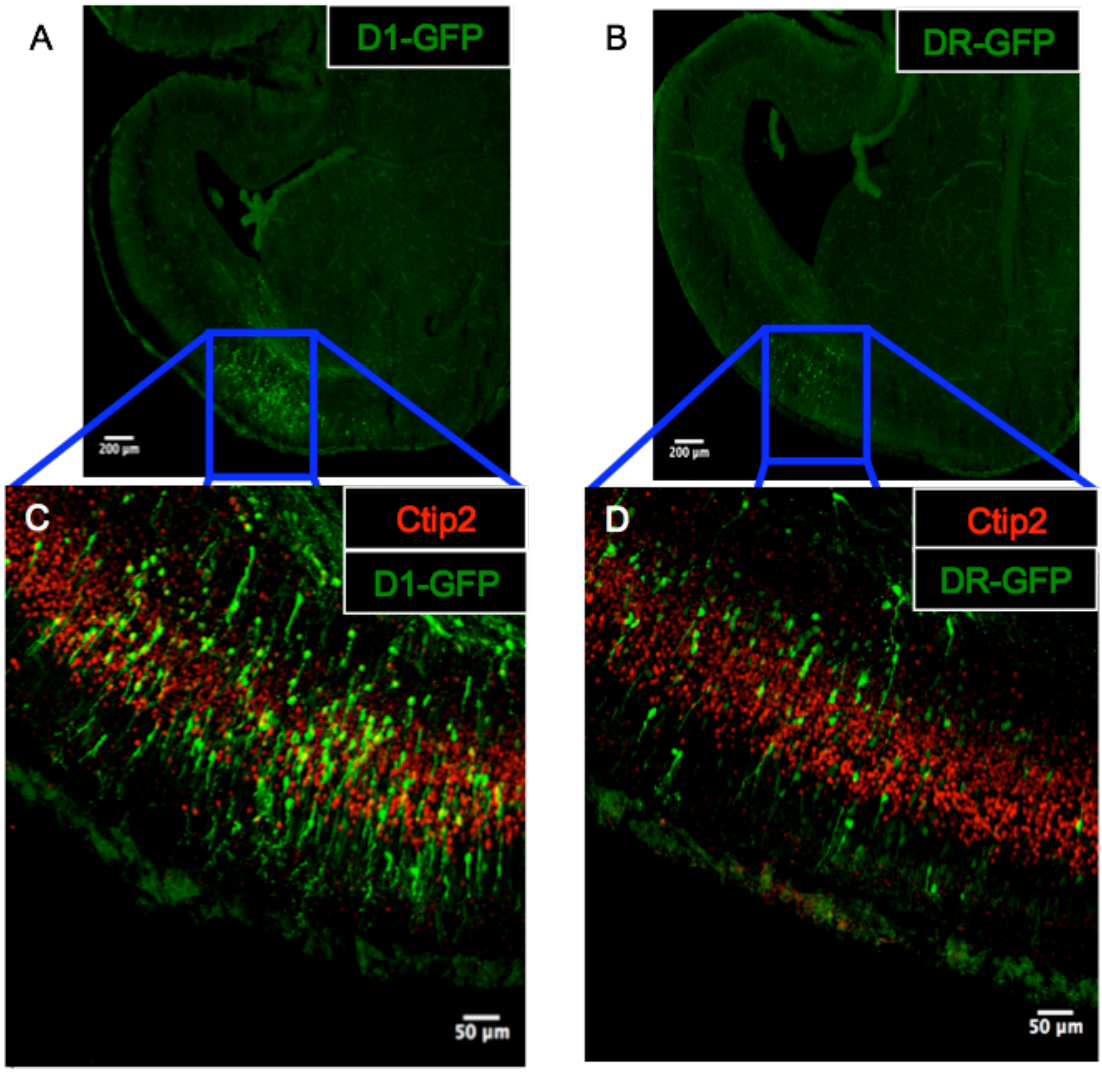

Figure 5. *Downregulation of endogenous dpy-19-1 causes increased rate of cortical migration.* Mouse embryos were electroporated *in utero* at E12.5, dissected and fixed at E16.5, cut into 40µm coronal sections, and processed for immunofluorescence with anti-Ctip2 (red), a marker for layer V cortical neurons, and anti-GFP (green). (A-B) Electroporation was performed to transfect neurons that would migrate to the cortex. (C-D) Cell position of D1- and DR-transfected cells was compared to the Ctip2 marker, which revealed an increased migratory rate in *dpy-19-1*-downregulating D1-positive cells.

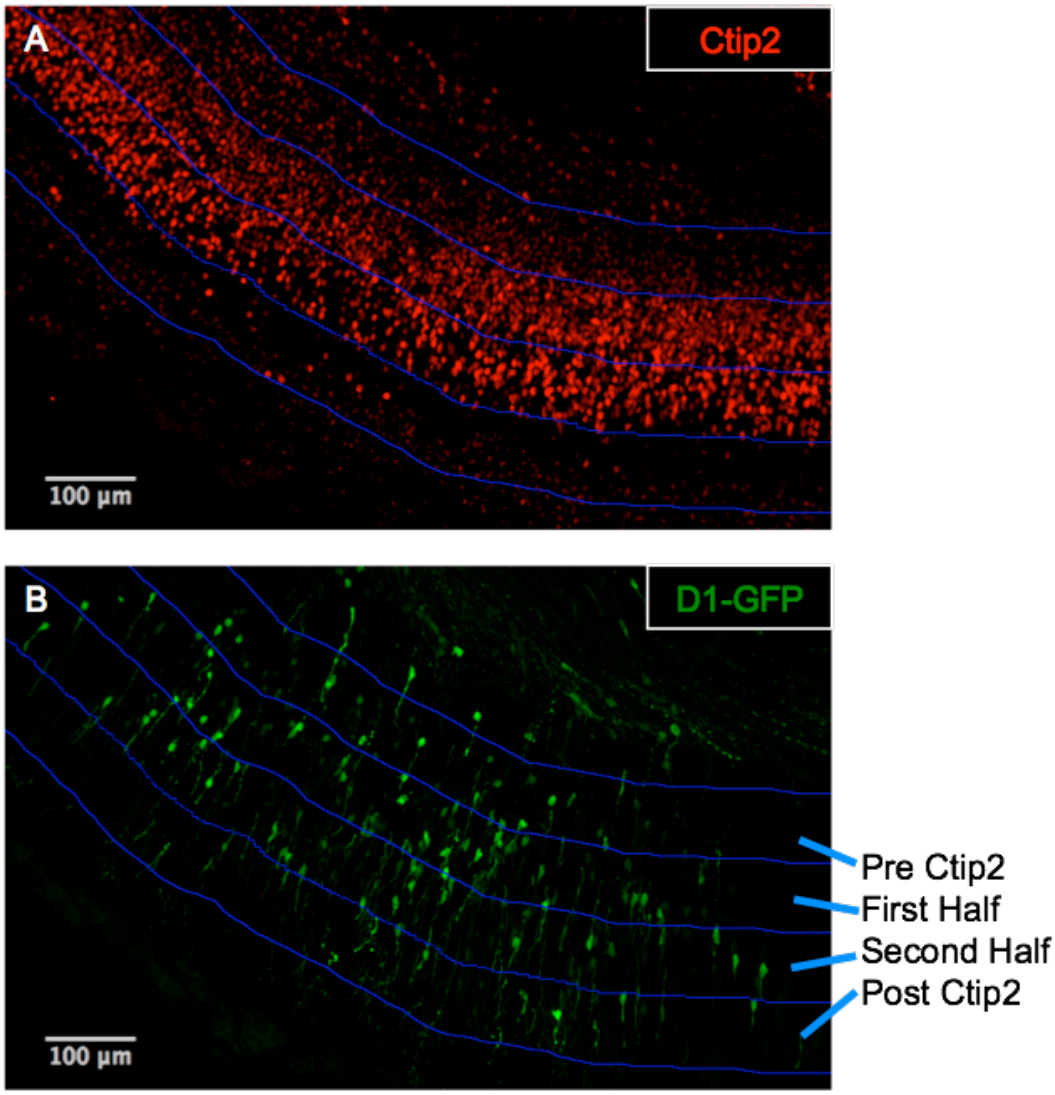

Figure 6. *Quantification method for downregulation of dpy-19-1 in migration.* (A) The Ctip2 layer was traced, and bands were created of equal width based on half the width of the Ctip2 band. (B) Cells were counted according to their band position. The first band was named Pre Ctip2, the next was the First Half of Ctip2, then Second Half of Ctip2, and the Post Ctip2 band. The quantification per band was reported as a percentage of the total cells counted in that 40µm slice.

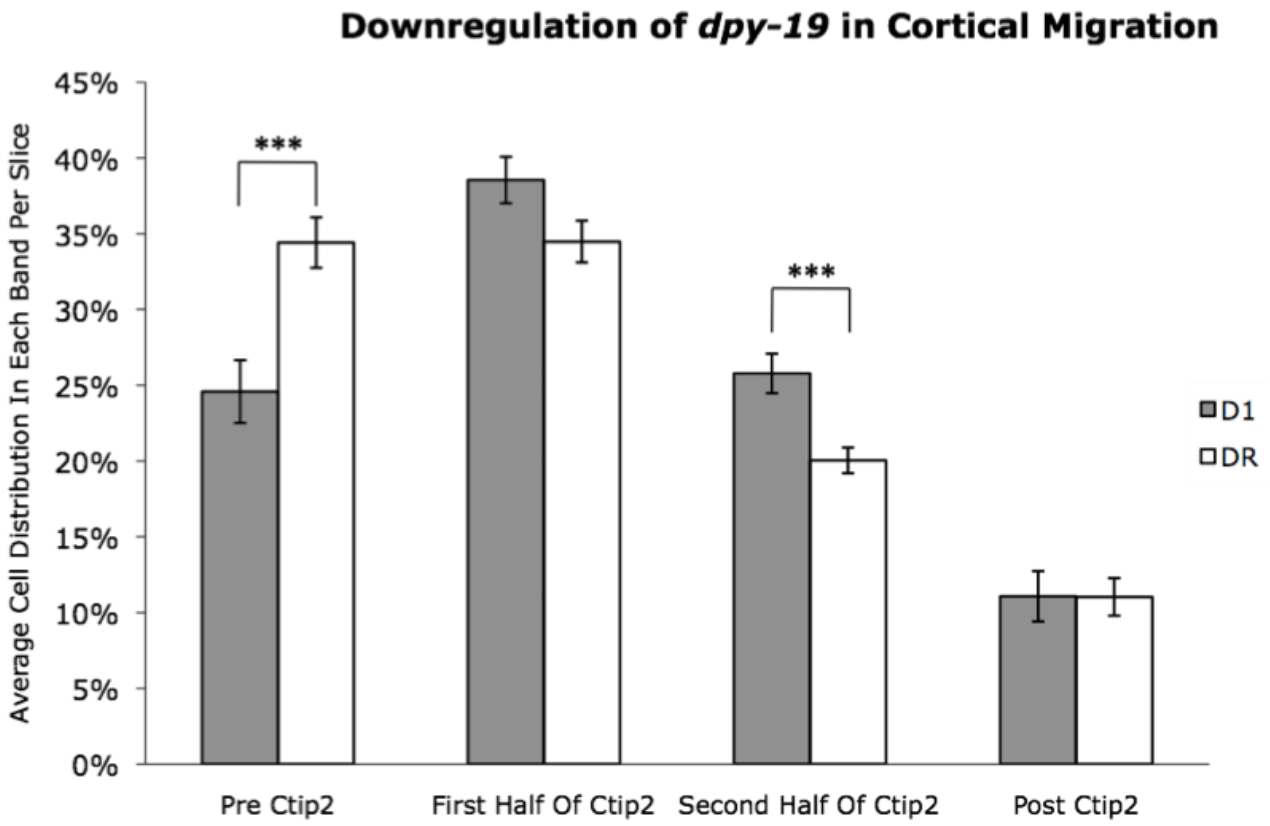

Figure 7. *Downregulation of dpy-19-1 affects rate of cortical migration.* D1-transfected cells were represented proportionally lower in the Pre Ctip2 band (p=0.0007), and proportionally higher in the Second Half of Ctip2 (p=0.0009). 2492 cells were quantified for D1 across 19 slices from 10 D1-electroporated embryo brains from 2 pregnant female mice. 2728 cells were quantified for DR across 23 slices from 7 DR-electroporated embryo brains from 2 pregnant adult female mice.

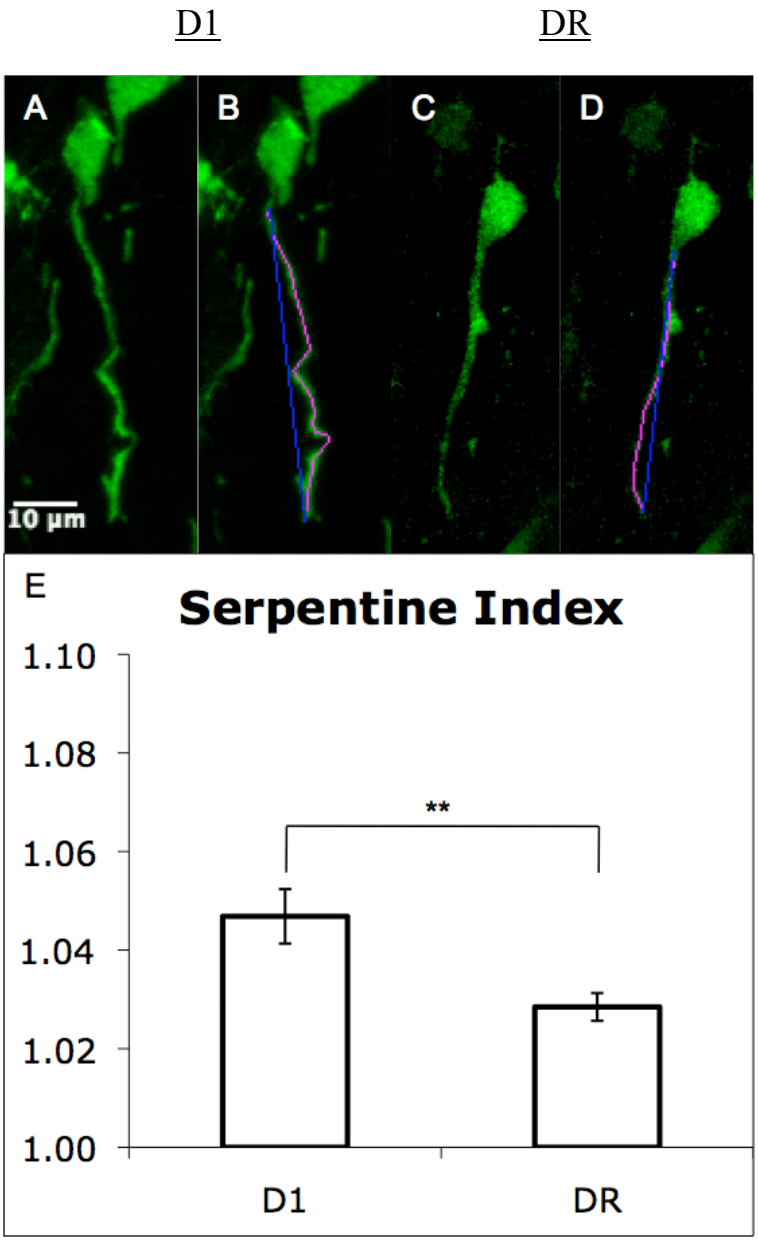

Figure 8. *Effect of dpy-19-1 downregulation on the morphology of the leading process in radially migrating cells.* The analysis of morphology was taken from pictures of the same *in utero* electroporated samples that were used for analysis of the migration. (A, C) Representative cells transfected with either D1 or DR, showing the serpentine morphology of D1 cells in the cortex. (B, D) The length of the leading process was measured using NeuronJ (magenta line), and divided by the distance between the end of the process and the beginning (blue line) to give the "serpentine index". (E) Quantification of the morphological data reveals a significant difference between D1 and DR ($p=0.0016$, Kruskal-Wallis test). 54 cells were analyzed from the D1 samples, and 36 cells from the DR.

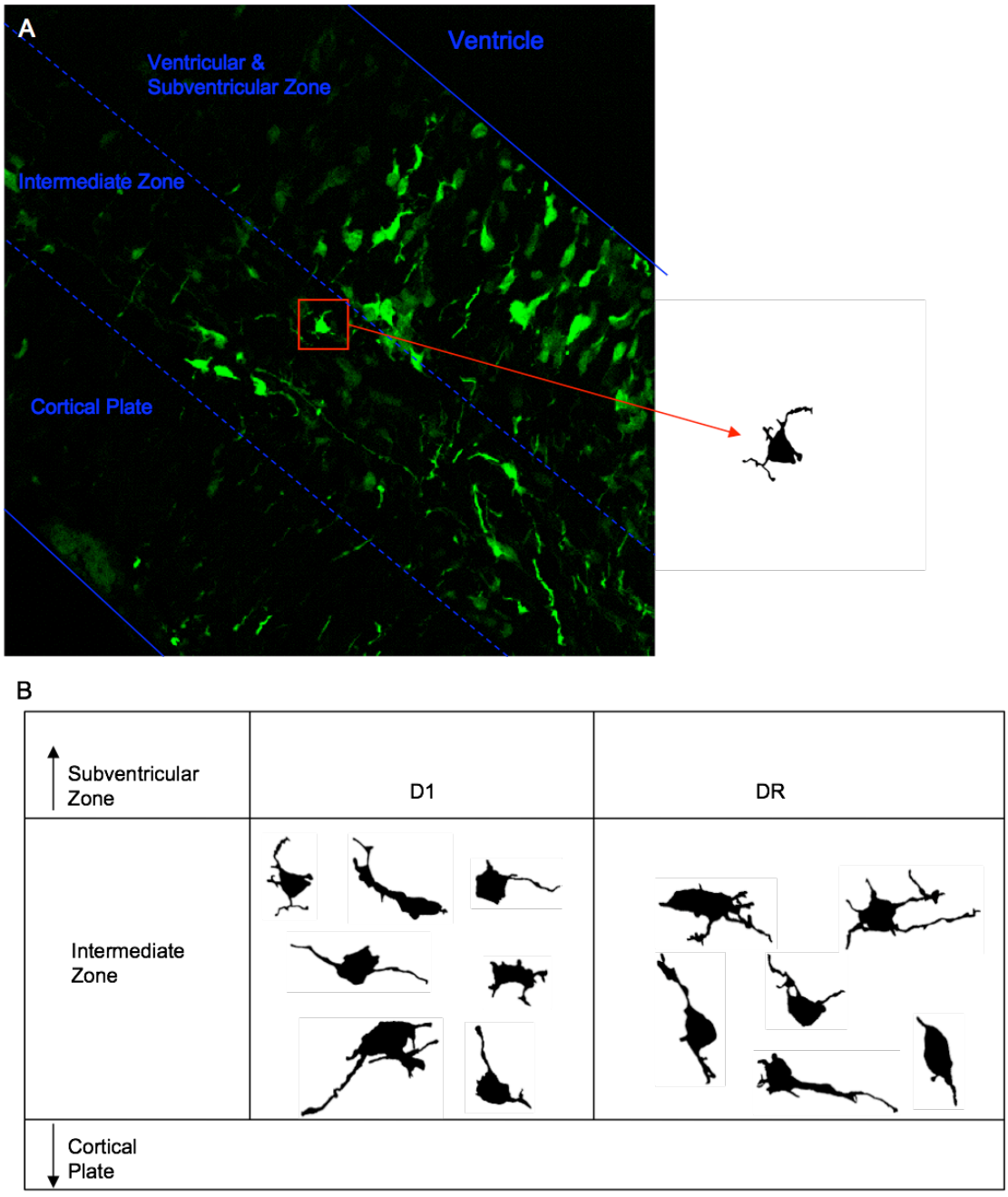

Figure 9. *Investigation of intermediate zone process branching related to dpy-19-1 downregulation.* Brains used for this experiment are the same ones that were used for Figure 4. (A) Traces were made of D1- or DR-positive cells from the intermediate zone at E14.5 to analyze their multipolarity. (B) Cells were rotated to orient them properly relative to an imagined shared subventricular zone and cortical plate. This method was used to determine whether the cells had an alteration in their ability to polarize, or in the number of neurites they developed.

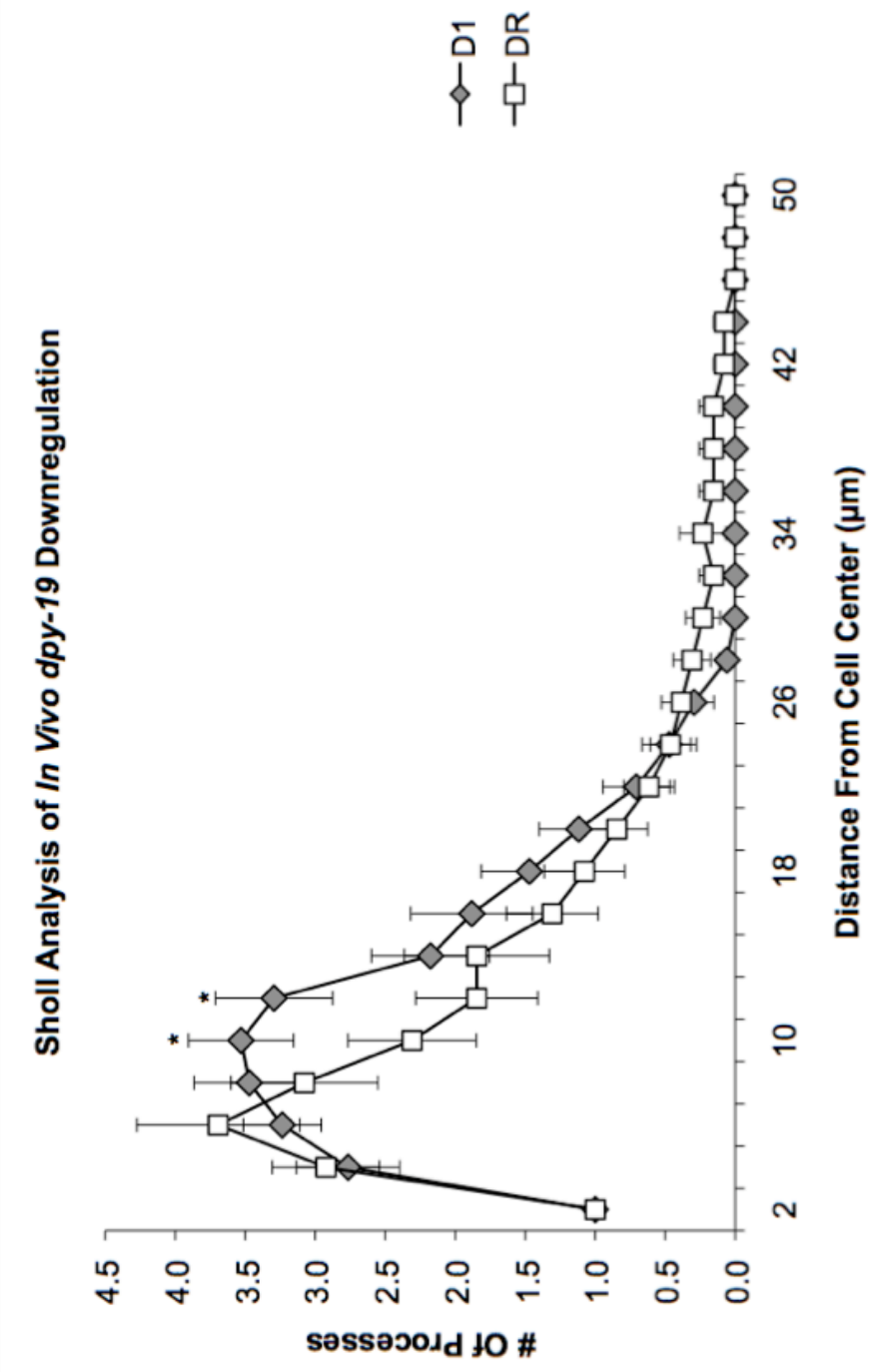

Figure 10. *Examination of the process development of cells with downregulated dpy-19-1.* Sholl analysis was performed to compare the amount of processes that were developed in the intermediate zone. Most points recorded no significant difference between the D1- and DR-transfected cells, only two points reported such a difference, at 10µm (p=0.0496, 2 tailed t test) and 12µm (p=0.0237) from the center of the cell (p=0.0237). 17 cells for D1, 6 brains, 1 pregnant adult mouse. 13 cells for DR, 5 brains, 1 pregnant adult mouse.

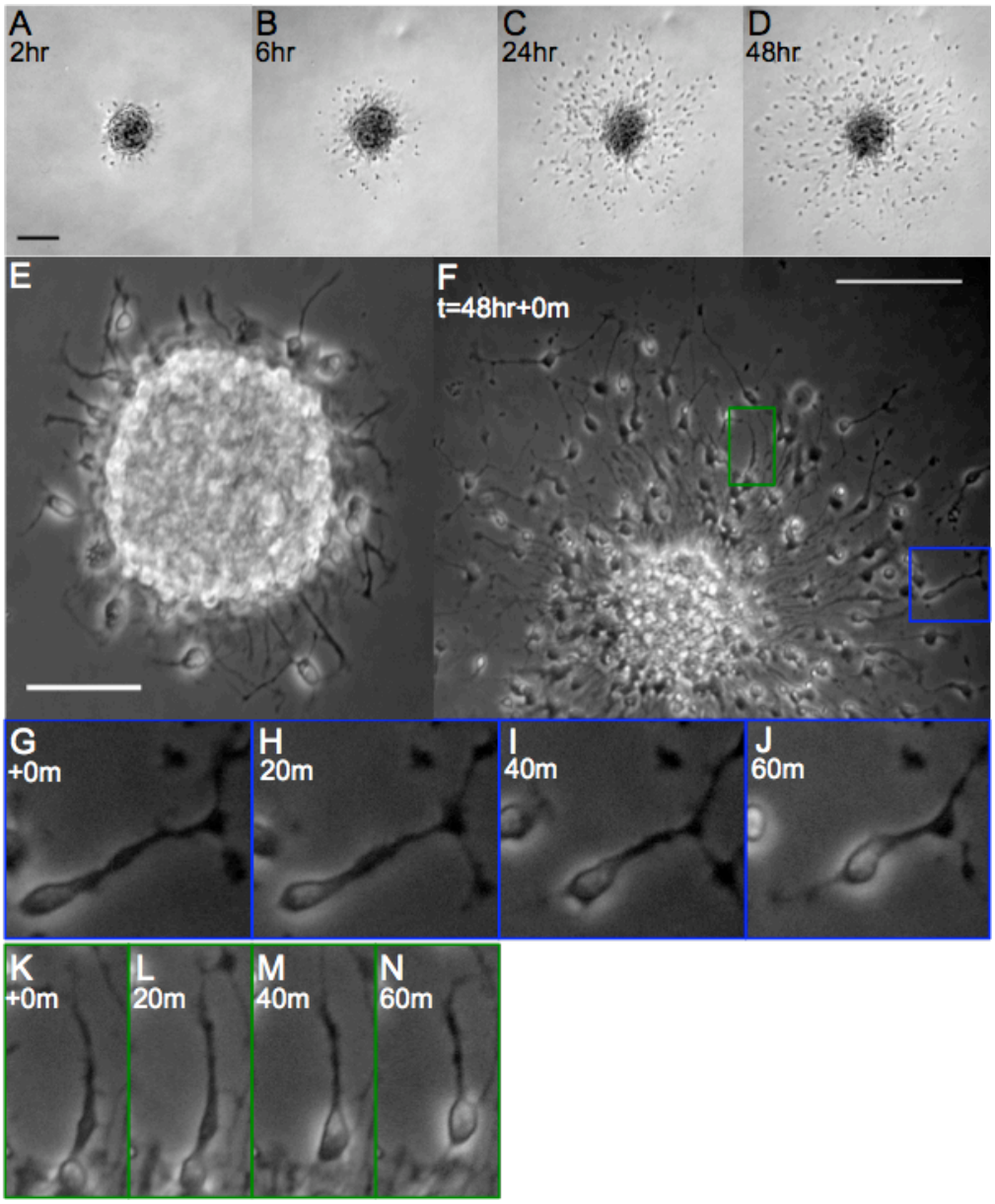

Figure 11. *Migration of untransfected neurospheres*. (A-D) Phase contrast images taken of an untransfected neurosphere after plating on coverslips coated with PDL and laminin. Images were taken at 2 hours, 6 hours, 24 hours and 48 hours. Scale bar represents 100µm. (E) Phase contrast image of an untransfected neurosphere taken at 20x magnification 2 hours after plating to show initial process extension and the beginning of outward migration. Scale bar represents 50µm. (F) Untransfected neurosphere after 48 hours of migration. Images of this neurosphere were taken every minute for 1 hour. Scale bar represents 100µm. Cells that migrated exhibited translocation of their cell body, which is shown in magnified images of the blue box (G-J), and the green box (K-N). The timepoints shown in these series are at 48 hours + 0 minutes, 20 minutes, 40 minutes, and 60 minutes.

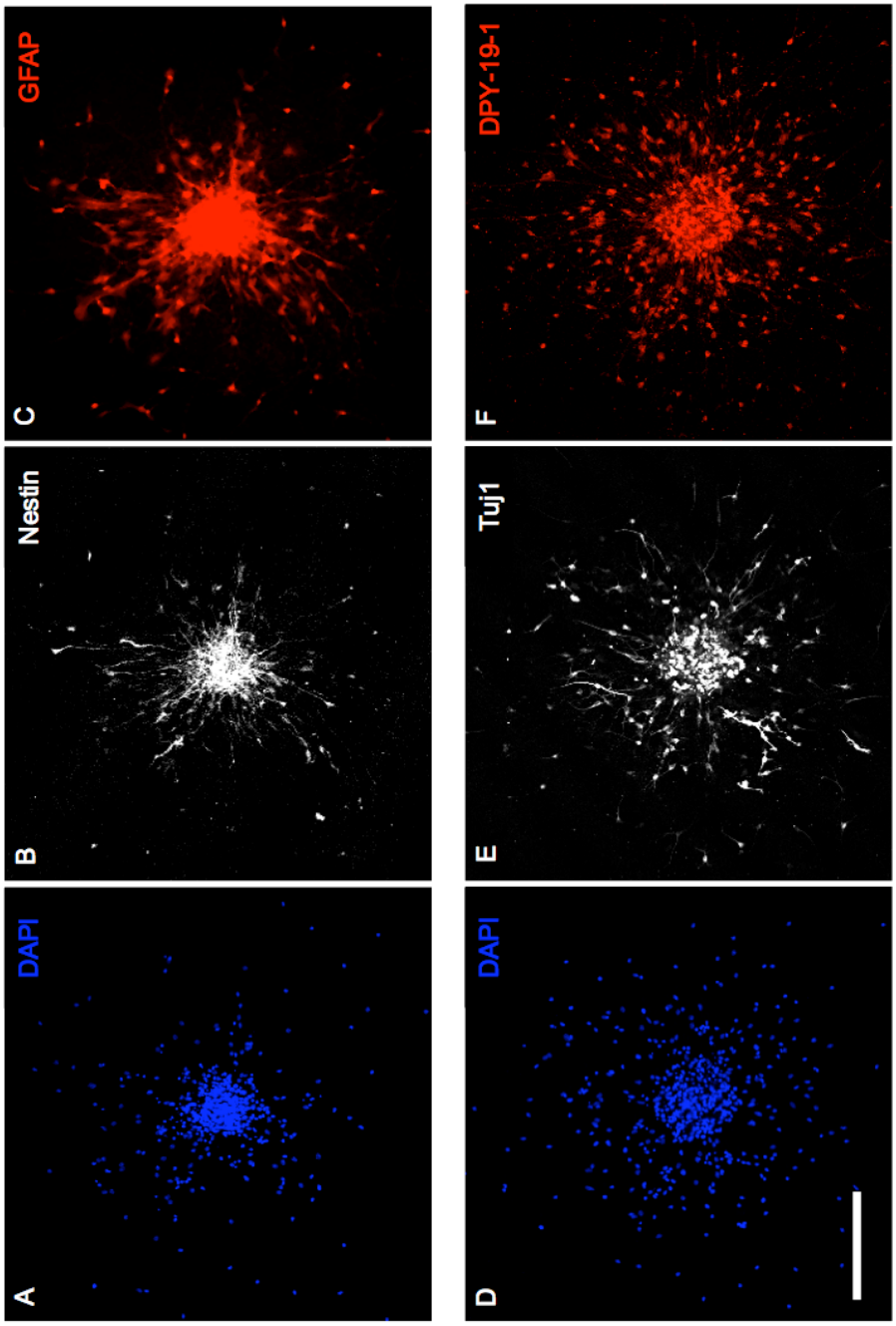

Figure 12. *Immunostaining of transfected migrating neurospheres.* (A-C) A Psuper transfected neurosphere stained with DAPI (blue), mouse anti-Nestin (white), and rabbit anti-GFAP (red). (D-F) A DR transfected neurosphere stained with DAPI (blue), mouse anti-Tuj1 (white), and rabbit anti-DPY-19-1 (red). Scale bar represents 200µm.

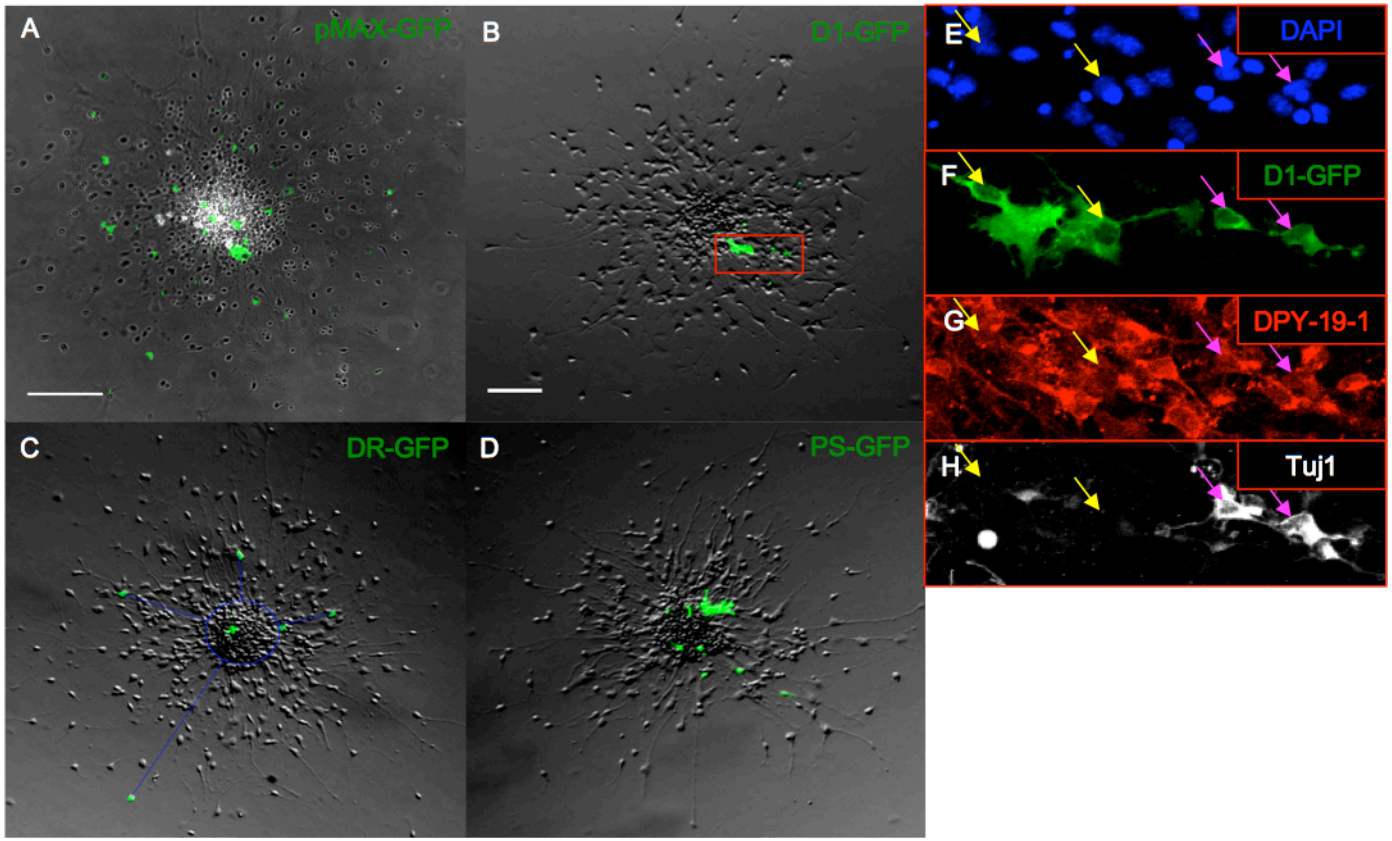

Figure 13. *Migration of transfected neurospheres*. (A) 10X phase contrast imaging of pMAXGFP transfected neurosphere, merged with fluorescent imaging of GFP signal shown in green. Scale bar represents 100µm. (B) 5X DIC imaging of D1 transfected neurosphere. Scale bar represents 100µm. The immunostaining of the red box is shown in (E-H). (C) 5X DIC imaging of DR-transfected neurosphere, showing the method of quantification of GFP-positive cell migration. Blue lines were generated using ImageJ to show the distance measured for each cell, starting from the edge of the central neurosphere mass. (D) 5X DIC imaging of PsuperGFP-transfected neurosphere. (E-H) D1-positive cells from (B) stained with DAPI (blue), goat anti-GFP (green), rabbit anti-DPY-19-1 (red), and mouse anti-Tuj1. Yellow arrows point to non-Tuj1 positive migrating cells, and magenta arrows point to Tuj1 positive migrating cells.

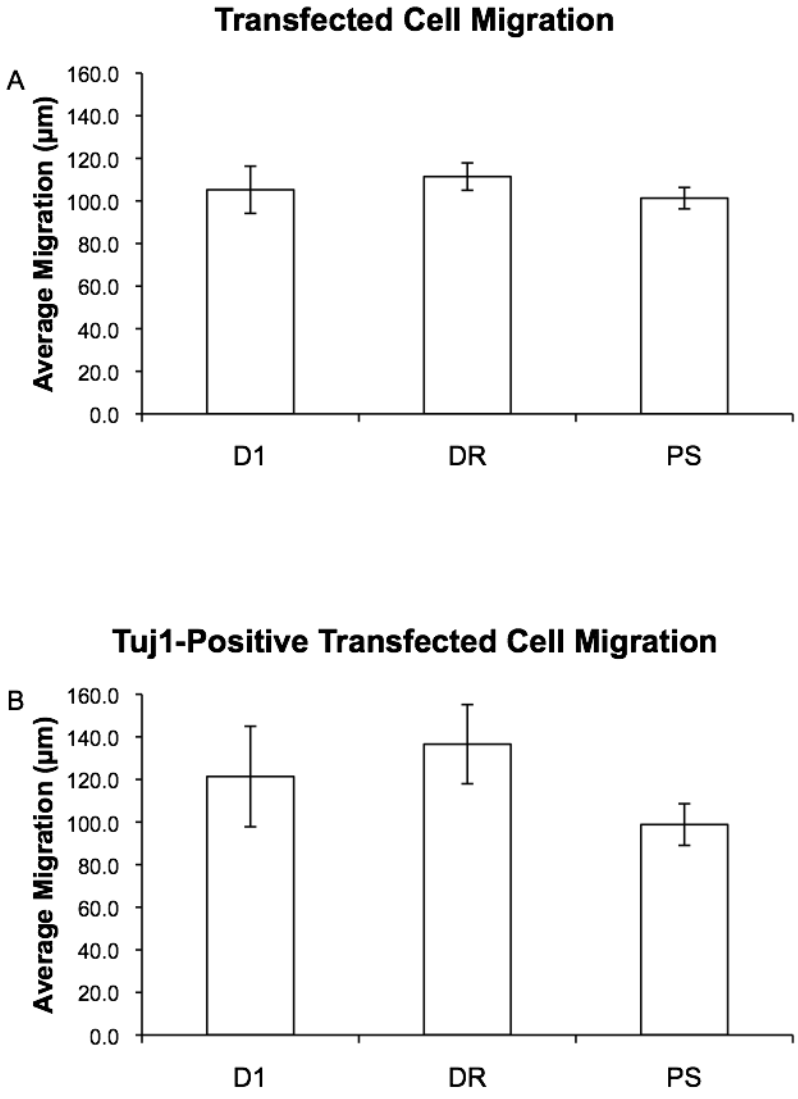

Figure 14. *Results of neurosphere migration assay.* (A) Quantification of distance migrated in all GFP-labeled cells. None of the groups showed a significant difference from any other. The sample size from D1 was 54 cells across 26 neurospheres from 4 separate rounds of nucleofection. DR had a sample size of 111 cells, 24 neurospheres, and 4 rounds of nucleofection. PS had a sample size of 155 cells, 24 neurospheres, and 4 rounds of nucleofection. (B) Quantification of distance migrated in GFP- and Tuj1-positive cells. None of the groups showed a significant difference from any other. The sample size from D1 was 13 cells across 3 rounds of nucleofection that were stained for Tuj1. DR had a sample size of 22 cells, PS had a sample size of 47 cells.

Table 1. *Neurosphere migration data.* Data from the neurosphere migration experiments broken up by rounds. Each round is labeled by the date it was plated. Only three rounds could be counted in the Tuj1 positive experiment because those are the rounds that were stained for Tuj1.

A.

	# of Cells	Avg. GFP-+ Cell Migration (μm)
4/1/2010 D1	10	110.7
4/1/2010 DR	14	89.5
4/1/2010 PS	25	87.8
4/30/2010 D1	15	87.5
4/30/2010 DR	42	134.0
4/30/2010 PS	53	98.1
5/5/2010 D1	19	106.9
5/5/2010 DR	23	85.1
5/5/2010 PS	42	115.8
5/8/2010 D1	10	123.4
5/8/2010 DR	32	110.3
5/8/2010 PS	35	98.3

B.

	# of Cells	Avg. Tuj1-Positive Cell Migration (μm)
4/30/2010 D1	5	64.7
4/30/2010 DR	6	219.4
4/30/2010 PS	18	65.0
5/5/2010 D1	4	148.5
5/5/2010 DR	1	73.4
5/5/2010 PS	15	129.9
5/8/2010 D1	4	165.2
5/8/2010 DR	15	107.6
5/8/2010 PS	14	109.0

REFERENCES

Austin, C., and Cepko, C. (1990). Cellular migration patterns in the developing mouse cerebral cortex. Development 110: 713-732.

Durbec, P., Franceschini, I., Lazarini, F., Dubois-Dalcq, M. (2008). In vitro migration assays of neural stem cells. Methods Mol Biol 438: 213-225.

Edmondson, J. C., and Hatten, M. E. (1987). Glial-guided granule neuron migration in vitro: a high-resolution time-lapse video microscopic study. J Neurosci 7: 1928-1934.

Guerrier, S., Coutinho-Budd, J., Sassa, T., Gresset, A., Jordan, N. V., Chen, K., Jin, W. L., Frost, A., Polleux, F. (2009). The F-BAR domain of srGAP2 induces membrane protrusions required for neuronal migration and morphogenesis. Cell 138: 990-1004.

Gupta, A., Sanada, K., Miyamoto, D. T., Rovelstad, S., Nadarajah, B., Pearlman, A. L., Brunstrom, J., and Tsai, L.H. (2003). Layering defect in p35 deficiency is linked to improper neuronal-glial interaction in radial migration. Nat Neurosci 6: 1284-1291.

Harris, J., Honigberg, L., Robinson, N., and Kenyon, C. (1996). Neuronal cell migration in *C. elegans*: regulation of Hox gene expresssion cell position. Development 122: 3117-3131.

Haydar, T. F., Bambrick, L. L., Krueger, B. K., Rakic, P. (1999). Organotypic slice cultures for analysis of proliferation, cell death, and migration in the embryonic neocortex. Brain Res Protoc 4(3): 425-37.

Honigberg L., and Kenyon C. (2000). Establishment of left/right asymmetry in neuroblast migration by UNC-40/DCC, UNC-73/Trio and DPY-19 proteins in *C. elegans*. Development 127: 4655-4668.

Jacques, T. S., Relvas, J. B., Nishimura, S., Pytela, R., Edwards, G. M., Streuli, C. H. ffrench-Constant, C. (1998). Neural precursor cell chain migration and division are regulated through different β1 integrins. Development 125: 3167-3177.

Kwiatkowski, A. V., Rubinson, D. A., Dent, E. W., Edward van Veen, J., Leslie, J. D., Zhang, J., Mebane, L. M., Philippar, U., Pinheiro, E. M., Burds, A. A., Bronson, R. T., Mori, S., Fässier, R., Gertler, F. B. (2007). Ena/VASP is required for neuritogenesis in the developing cortex. Neuron 56: 441-455.

Leslie A. King, "A role for murine dumpy-19 in neocortical development" (PhD dissertation, Pritzker School of Medicine, 2006): 60-66.

Liu, X. S, Chopp, M., Zhang, R. L., Hozeska-Solgot, A., Gregg, S. C., Buller, B., Lu, M., Zhang, Z. G. (2009). Angiopoietin 2 Mediates the Differentiation and Migration of Neural Progenitor Cells in the Subventricular Zone after Stroke. J Biol Chem 284(34): 22680-9.

Marin, O., and Rubenstein, J. L. (2001). A long, remarkable journey: tangential migration in the telencephalon. Nature Rev Neurosci 2: 780-790.

Marin, O, and Rubenstein, J. L. (2003). Cell migration in the forebrain. Annual Review of Neuroscience 26: 441-483.

Ocbina, P. J., Dizon, M. L. V., Shin, L., Szele, F. G. (2006). Doublecortin is necessary for the migration of adult subventricular zone cells from neurospheres. Mol Cell Neurosci 33: 126-135.

Ohshima, T., Hirasawa, M., Tabata, H., Mutoh, T., Adachi, T., Suzuki, H., Saruta, K., Iwasato, T., Itohara, S., Hashimoto, M., Nakajima, K., Ogawa, M., Kulkarni, A. B., Mikoshiba, K. (2007). Cdk5 is required for multipolar-to-bipolar transition during radial neuronal migration and proper dendrite development of pyramidal neurons in the cerebral cortex. Development 134: 2273-2282.

Pevny, L., and Rao, M. S. (2003). The stem-cell menagerie. Trends in Neurosciences 26(7): 351-359.

Salser, S., and Kenyon, C. (1992). Activation of a *C. elegans Antennapedia* homolog within migrating cells controls their direction of migration. Nature 355: 255-258.

Tanaka, T., Serneo, F. F., Tseng, H. C., Kulkarni, A. B., Tsai, L. H., Gleeson, J. G., (2004). Cdk5 phosphorylation of doublecortin ser297 regulates its effect on neuronal migration. Neuron 41: 215-227.